Experimental and Numerical Wear Characterization by Means of Active Thermography Technique

Experimental and Numerical Wear Characterization by Means of Active Thermography Technique

Luca Corsaro, Edoardo Goti, and Francesca Curà(✉)

Department of Mechanical and Aerospace Engineering, Politecnico di Torino, Corso Duca degli Abruzzi 24, 10129 Torino, Italy
francesca.cura@polito.it

Abstract. Thermography is a non-contact technique used to obtain thermal maps of a component surface. Active Thermography (AT) has gained a lot of interest in recent years as a tool to characterize thermal properties and fatigue damage in materials, coatings, and components. Hidden flaws can also be detected based on the surface thermal map in a non-destructive way . This paper presents a preliminary experimental procedure where Lock-in AT is exploited to characterize wear damages of a flat steel surface featuring a series of linear wear traces from pin-on-flat wear tests. A dedicated temperature data processing route was set up to correlate thermal signals to the characteristic parameters which may identify the amount of material loss by wear. The results suggest that AT may be a promising, fast, and alternative method to detect and quantify wear on surfaces. An exponential law correlates the wear track width, depth, and area with the intensity peaks of the fundamental harmonics of the pulsed thermal response. Although the sensitivity and reliability of this method is still to be assessed, this preliminary work might pave the way to significant implications for AT in industry in the case of wear on hidden surfaces.

Keywords: wear · Lock-In · Active Thermography

1 Introduction

Wear phenomena represents one of the most relevant damages in mechanics. In the scenario of Industry 4.0, the quantification of the amount of wear and the wear control in components is becoming a relevant issue to support industrial process optimization.

Thermography is a non-contact technique that can be used to obtain thermal maps of a component surface during a given observation period. In the technical literature of recent years, many efforts have focused on thermographic testing methods as a tool to characterize the fatigue damage in materials, coatings and components. More recently, Active Thermography (AT), also called “stimulated thermography” became attractive for a variety of manufacturing processes. This technique requires that surfaces are thermally stimulated by means of an external heat source in order to characterize thermal properties and/or to detect flaws based on the thermal map. The thermal stimulation can

F. Concli et al. (Eds.): ISIEA 2024, LNNS 1124, pp. 133–142, 2024.
https://doi.org/10.1007/978-3-031-70462-8_13

be concentrated or diffused, for instance, laser beam stimulation, flash photo-thermal stimulation, induction stimulation, and electromagnetic or ultrasound stimulation. Many papers describing methods and algorithms to improve hidden defects visibility have been published [1] [2] [3] [4] [5]. Active thermography is well-suited for detecting surface and subsurface defects because the thermal response of a component volume with a defect is different than in sound regions. For instance, active thermography has been successfully applied in the offline investigation of the welding microstructure and defects [6] and in [7] [8] some algorithms related to phase map results were exploited to evaluate both crack growth and possible crack tip location. In case of materials characterization, an Active Thermography setup was recently and successfully developed to estimate thermal diffusivity values of thermal barrier coatings (TBCs) [9] [10] and Aerogel materials [11], according to ISO 18555 and ISO 18755 Standards. To that aim, both pulsed and Lock-In configurations were adopted. In [12] Passive (without thermal excitation) and Active (with thermal excitation) Thermography approaches were adopted to characterize specimens subjected to High Cycle tests, in order to relate the thermal diffusivity variation of each sample to the corresponding variation of traditional parameters as surface thermal increment and hysteresis loop area.

This paper explores a preliminary experimental procedure where AT is proposed to characterize wear damages. The AT analysis is here applied to measure the stimulated temperature map of a flat steel surface featuring a series of exposed wear traces. A dedicated temperature data processing route was set up and allowed to correlate thermal signals to the characteristic parameters which identify the amount of material loss by wear, e.g. the wear track depth and width, and the cross-sectional wear track area.

Sine wear phenomena are complex to investigate, several standards and custom testing methods are currently exploited in laboratory practice [13, 14]. Amongst the other standard model tests, pin-on-flat is a well-established and widespread wear test method for research purposes [15]. Reciprocating pin-on-flat tests were carried out in this work to produce wear traces of increasing size on the flat sample analyzed by AT.

The results presented in this study suggest that AT may be a promising way to inspect worn-out surfaces. However, further refinements are needed, and the sensitivity and reliability of this method is still to be assessed through a systematic test campaign with different materials and damaged regions of different size and shapes.

This procedure is intended to be a fast method, alternative to the traditional ones which exploit surface topographic data or surface profiles. The method is here introduced in the case of exposed wear tracks, but it might open up to significant implications for industry if it is extended to the identification or quantification of wear damages on hidden surfaces.

2 Materials and Methods

Tribological tests were carried out by means of a TRB pin-on-disk tribometer (Anton Paar TriTec, CH) with a rectangular 4 mm thick C45 steel sample (AISI 1045). A 10 mm diameter alumina sphere was used as the friction partner for pin-on-flat tests. Wear tests were performed in linear reciprocating mode with the ball installed in a stationary ball-holder and the sample was fixed to a sliding table, according to the ASTM G133 standard.

The test load was 10 N, and the reciprocating motion occurred with frequency of 2 Hz. The stroke length was 12mm corresponding to a maximum speed of about 0.1m/s in the middle of the stroke. A series of 11 tests were performed in sequence with increasing sliding distance from 2 m to 1000m, herein referred to as Track n.1 to n.11, to obtain wear scars of increasing size. A fresh location on the sphere was exposed before starting each test. The profiles of wear tracks were measured by stylus profilometry (SM Instruments PGS200, IT) according to the scheme in Fig. 1. One single profile was acquired in the middle of the stroke at the end of the series of test. The corresponding representative quantities describing the size of the wear track, i.e., width, depth and cross-sectional area, are listed in Table 1. The same zone was used during the active thermography measurements.

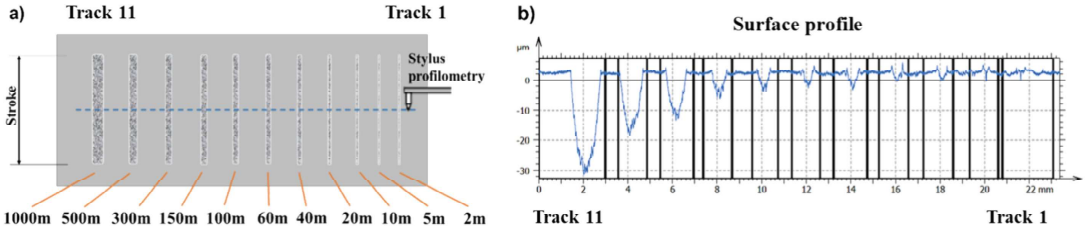

Fig. 1. (a) Schematic of the test sequence and profile extraction; (b) Wear track profile acquired by stylus profilometry of the sample surface at the end of the series of test.

Table 1. Characteristic wear parameters of the wear tracks obtained from the profilometric inspections. Data refer to the middle of the stroke.

Track n°	Sliding distance [m]	Width [mm]	Depth [μm]	Cross-sectional Area [μm^2]
1	2	0,261	4,32	398
2	5	0,432	5,40	656
3	10	0,432	3,67	739
4	20	0,492	3,70	893
5	40	0,565	4,65	1135
6	60	0,592	5,29	1141
7	100	0,567	7,60	1950
8	150	0,640	8,53	2748
9	300	0,926	15,49	8544
10	500	1,060	18,70	12379
11	1000	1,355	34,49	30138

Wear characterization was performed by means of the Active Thermography (AT) equipment from JTech Lab at Politecnico d Torino. It is composed of an IR camera, a laser beam excitation source and a PC control unit. The IR camera is a FLIR A6751sc with sensitivity lower than 20 mK and 3–5 μm spectral range, while the laser source can generate a maximum power of 50 W concentrated in a small surface.

Lock-In Active Thermography technique in reflection mode configuration (see Fig. 2) was adopted in this activity. A periodic heating was generated on the component surface and thermal maps in terms of response amplitude or phase were acquired. This way, possible heat conduction alterations due to surface or subsurface damage can be pointed out in a qualitative or quantitative way. Amplitude and phase images were extracted at the so-called Lock-In frequencies; these frequencies were chosen due to the high energy contribution in the frequency domain.

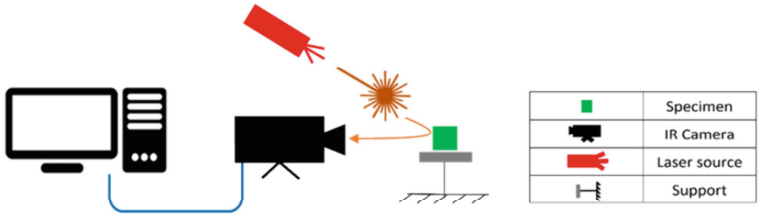

Fig. 2. Schematic of the active thermography equipment.

Lock-In frequencies depend on the waveform of the thermal power signal and represent a kind of resonant thermal frequencies of the system. In case of a sine wave power excitation, only the first Lock-In frequency is considered, and it is computed with the corresponding period excitation. In this work, a square thermal power wave with a duty cycle equal to 50% was considered to heat up the worn-out regions of the flat sample. In literature, three Lock-In frequencies are usually considered in case of a square wave excitation, and they correspond to the odd harmonics (i.e., I harmonic - I Lock-In frequency, III harmonic - II Lock-In frequency and V harmonic - III Lock-In frequency.). The real square wave frequency response may introduce amplitude or phase contributions also at different harmonics (for example II or IV harmonic), but they are not considered as Lock-In frequencies due to the low energy level [16]. In this work, more than the two fundamental harmonics (I-III harmonics) were investigated. A dedicated analysis to the II harmonic was also performed to investigate if the wear superficial damage can be detected by using that harmonic since its contribution was no negligible in our experiments.

In this activity, each wear track was thermally excited in the middle of the stroke through a pulse train of 20 heating pulses with period of 10 ms and a power of 20 W. The specimen was located 790 mm away from the IR camera and the frame rate acquisition was 785,7 Hz. Repeatability was checked with 8 test repetitions. Each repetition was carried out after the complete cooling-down of the sample surface.

An alternative Lock-In data interpretation was proposed with respect to the well consolidated approach proposed in the scientific literature. Frequency response of each pixel is usually evaluated from the time-domain temperature profile, and results (amplitude and phase images) are extracted at the Lock-In frequencies. In this study, radiance values were extracted instead of temperature from each pixel. This way, emissivity computation was avoided in the very small area of the wear tracks, due to the same surface aspect of wear traces. An average radiance curve was evaluated over a Region Of Interest (ROI) located in the center of each wear track (see Fig. 3) by averaging the radiance values from each pixel within the ROI. For the present investigation a ROI of same dimension

was chosen in order to highlight the effect of the increasing size of the wear track. The surface outside the wear track can be considered as a sound region. Therefore, when the width of the wear track increases, the share of the ROI covered by a sound region is reduced.

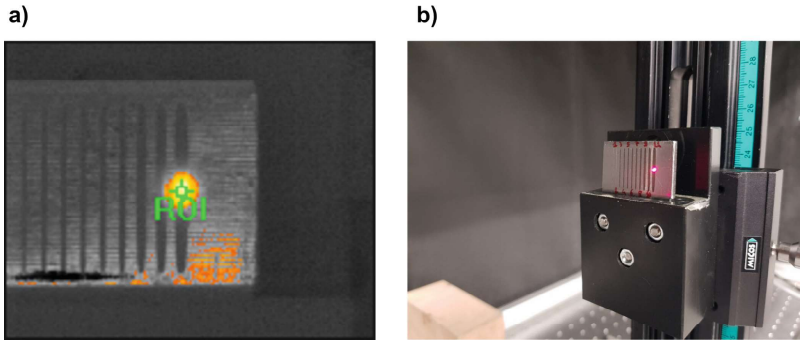

Fig. 3. (a) ROI; (b) test setup where the specimen and the laser pointer is visible.

The given ROI was the same in terms of number of pixels for each wear track; it was located in the center of the stroke where the laser was applied. Data extracted were processed with FLIR ResearchIR® software considering the evolution of the environmental parameters (temperature, humidity and reflected temperature) which were monitored during the tests.

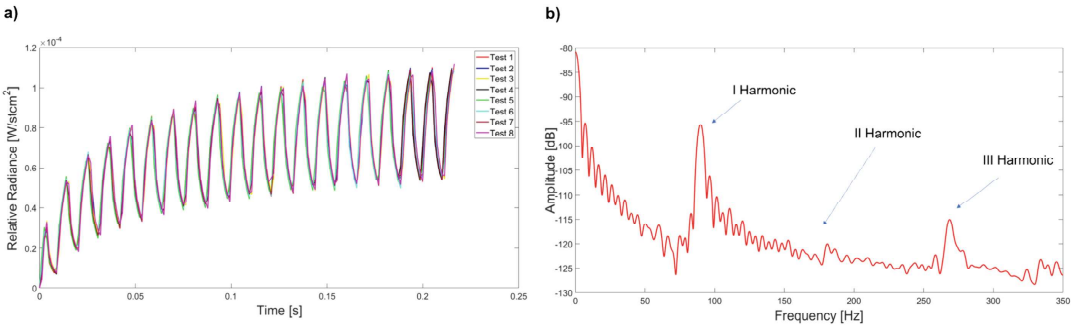

Fig. 4. (a) Relative radiance profiles; (b) Amplitude power spectrum.

The relative radiance profiles (absolute radiance profiles with respect to the environmental radiance) for each test repetition is illustrated in Fig. 4 (a), as an example for wear track n°6. Signal Processing Toolbox 8.6 (available in Matlab Software) was exploited to compute the power spectrum of the frequency response. Amplitude in Decibel was preferred to emphasize differences between the peaks of the thermal responses (see Fig. 4b). Particular attention to the spectral leakage was also devoted. As suggested in the Matlab guideline [17], the leakage value directly impacts on the mainlobe width through the Kaiser window. Data were processed with a rectangular window to improve spectral resolution (leakage value equal to 1). Results in terms of amplitude for the first three harmonics (see Fig. 4 (b)) were extracted, and a mean value for each wear track

over the 8 repetitions was considered. These results from AT analysis were correlated with the wear parameters of Table 1 with an exponential fitting. Equation (1) shows the mathematical formulation adopted for each harmonic:

$$WP = a \bullet e^{bc} \tag{1}$$

where a and b are two coefficients to be determined, *WP* is the wear parameter (depth, width or area) and c is the peak value of the investigated harmonic. a and b coefficients were calibrated with the goal of maximizing the R^2 fitting index.

As illustrated in Fig. 1, wear tracks from n°1 up to n°5 show a very similar size and shape, therefore only the wear track n°4 was considered in the analysis.

3 Numerical Model

A numerical model of the laser heating process was set up for the same wear tracks analyzed in the experimental activity to validate the proposed wear characterization method. In excluded wear tracks (n°1, 2, 3, 5) no appreciable thermal responses variation was observed.

A 3D model was implemented. The steel specimen was defined as a rectangular prism whose dimensions are identical to the real sample, and just one wear track was modelled in the middle of the specimen for each case. The wear tracks were modelled in a simplified way by assuming a circular profile whose width and maximum depth were equal to the values reported in Table 1. A quarter geometry with symmetry conditions was exploited to reduce both number of elements and computational time.

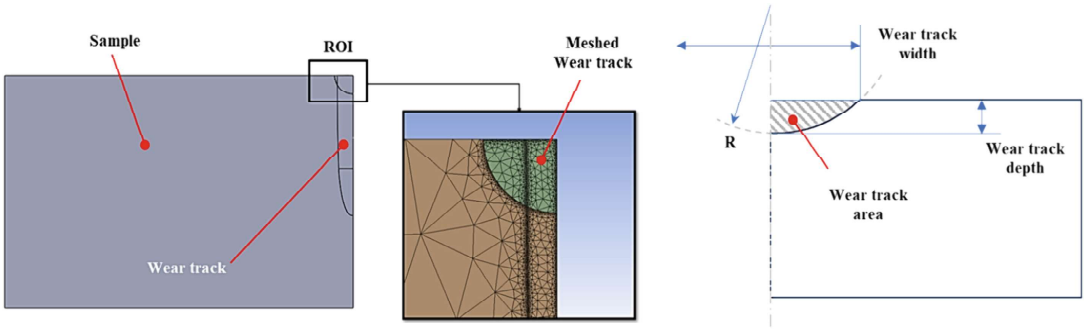

Fig. 5. Wear track n°7: geometry and mesh.

A Transient Thermal Analysis was setup through the Mechanical APDL solver in Ansys Workbench. Physical (density) and thermal (specific heat and thermal conductivity) properties of AISI 1045 (UNI C45) were defined over the computational domain from the Ansys Library. Pulsed heating was modelled with a Gaussian heat source to reproduce the laser beam excitation. Convective effects with air were utilized as boundary conditions.

A signal mean value was extracted from a ROI whose dimensions and location were identical to those adopted during the experimental analysis. Figure 5 shows, as an

example, the meshed domain of analysis in case of the wear track n°7. A finer tetrahedral mesh was defined inside the ROI (green region in Fig. 5), i.e. where the laser beam spot interacts with the steel surface. In this case, temperature profiles were obtained from each node instead of radiance values. Temperature profiles and wear track parameters were correlated following the same procedure explained in Sect. 2.

4 Results

Experimental and numerical results for tested wear tracks are presented in this section. Experimental and numerical frequency responses for the tested wear tracks (n°: 4, 6, 7, 8, 9, 10 and 11) are shown in Fig. 6.

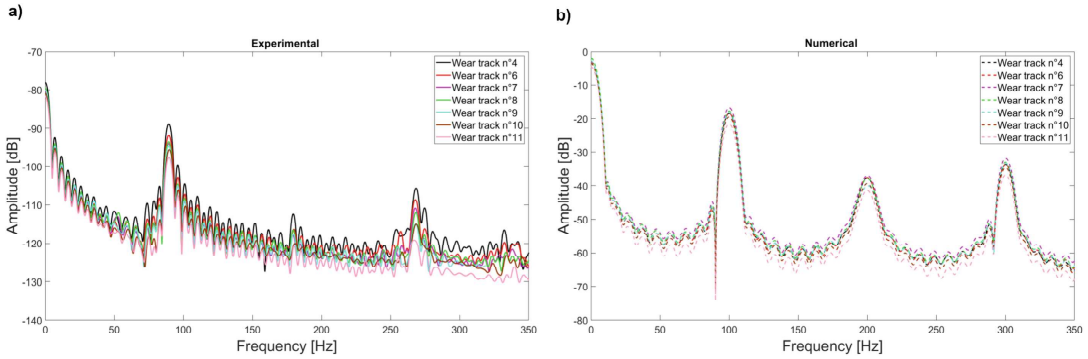

Fig. 6. (a) Experimental frequency response in radiance values; (b) numerical frequency response in temperature values.

From the experimental point of view, the analysis of Fig. 6 shows a different thermal response on the basis of the tested wear track. More in detail, thermal variations in terms of peaks amplitude, and for each harmonic, may be correlated with wear parameters (depth, width and area shown in Table 1). Figure 7a correlates the experimental peak amplitude from the AT responses with the wear tracks area. The correlation between peak amplitude values and the corresponding cross-sectional wear track area are indicated as dots, while the exponential fitting is represented by continuous lines. Sim-ilar results are illustrated in Figs. 8a and 9a, for wear track width and depth, respec-tively. Figures 7a to 9a shows that a sound correlation exists between the peak ampli-tude and the characteristic size and geometry of the wear tracks, which is also suggested by the high values of the R2 index (see Table 2).

From the numerical point of view, similar results can be pointed out in Figs. 7b to 9b. The correlation between the numerical peaks amplitude and the wear parameters (area, width and depth) follows the same approach proposed for the experimental correlation and dashed lines are used for the exponential fitting. Numerical results in terms of frequency responses variations are according to the experimental ones. Moreover, the decibel variation obtained for the I harmonic is comparable. The difference in terms of amplitude values is related to the original signal in time domain (radiance for experimental results and temperature for the numerical simulations).

Table 2. R2 indexes.

	Experimental			Numerical		
Wear parameter	I Harmonic	II Harmonic	III Harmonic	I Harmonic	II Harmonic	III Harmonic
Area	0.9782	0.9179	0.9847	0.9087	0.9417	0.9011
Width	0.8742	0.813	0.9457	0.7414	0.9083	0.7197
Depth	0.9754	0.8781	0.9916	0.8233	0.9257	0.8095

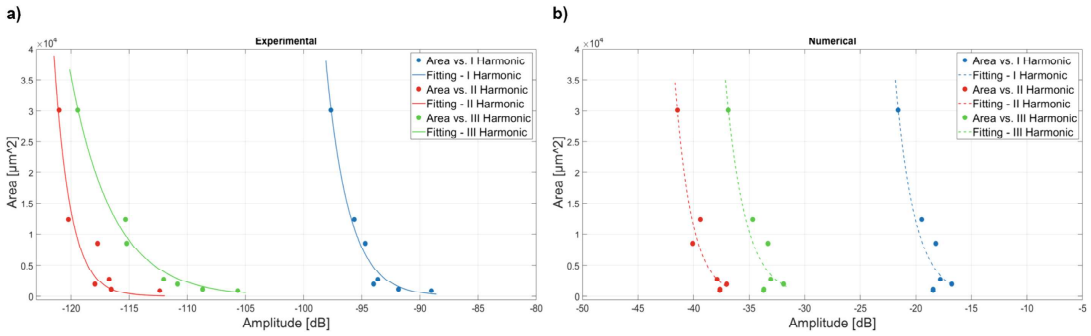

Fig. 7. (a) Area vs. experimental amplitude; (b) Area vs. numerical amplitude.

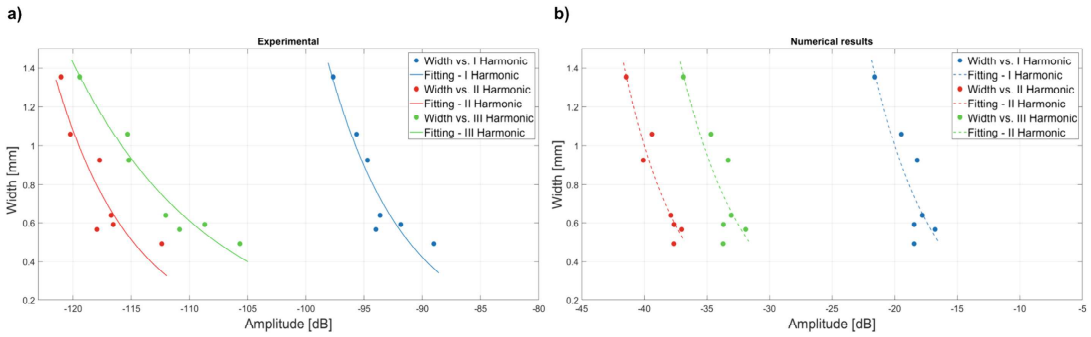

Fig. 8. (a) Width vs. experimental amplitude; (b) Width vs. numerical amplitude.

The R^2 index is listed in Table 2 for each exponential fitting. In particular, experimental correlations generate high R^2 index in case of I and III harmonics; while the same considerations are obtained for numerical results in case of I and II harmonics.

Furthermore, high experimental R^2 index were obtained, for each investigated harmonics, only with area and depth parameters.

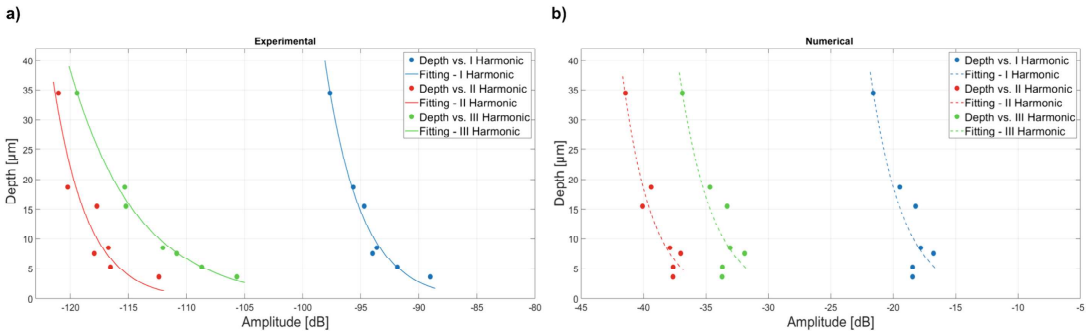

Fig. 9. (a) Depth vs. experimental amplitude; (b) Depth vs. numerical amplitude.

5 Conclusions

In this paper a flat steel sample featuring a series of wear track from pin-on-flat wear tests was inspected through Active Thermography. The results obtained in this preliminary work show that thermal response of a worn-out surface can correlate with the characteristic size of wear scars and, thus, with the amount of wear damage. The thermal response changed because the wear track affects the heat conduction into the material. Therefore, this preliminary analysis setup the basis for the future development of a Non-Destructive Technique (NDT) to estimate wear damage of surfaces.

The developed method, alternative to those illustrated in the literature for Lock-In data elaboration (amplitude images), uses the thermal response in the frequency domain with a dB scaling. This way, the difference among the amplitude resonances peaks at the fundamental harmonics is highlighted and related to the wear damage evolution. The best empirical damage law between thermal and traditional tribological parameters is represented by an exponential approximation featuring high R^2 indexes. Three fundamental harmonics were investigated, and the best wear characterization is achieved with the III harmonic.

Finally, results obtained in the numerical analysis are in agreement with the experimental wear characterization. Wear tracks modelled with a simplified geometry can reproduce the real wear track behavior. From the wear parameter point of view, area and depth were the wear indicator most closely correlated to the dynamic thermal signals from Lock-In Active Thermography.

In conclusion, the perspective of AT in real industrial practice is to quantify wear damage according to a non-contact and alternative method.

Acknowledgements. The authors would like to thank Daniele Lazzaroni for his help as part of his Batchelor thesis project.

References

1. He, Y., Tian, G., Pan, M., Chen, D.: Eddy current pulsed phase thermography and feature extraction. Appl. Phys. Lett. **103**(8) 2013
2. Larbi, W.B., Ibarra-Castanedo, C., Klein, M., Bendada, A., Maldague, X.: Experimental comparison of lock-in and pulsed thermography for the nondestructive evaluation of aerospace materials. In 6th International Workshop, Advances in Signal Processing for Non Destructive Evaluation of Materials (IWASPNDE), Ontario, Canada. Citeseer (2009)
3. Liu, J., Yang, W., Dai, J.: Research on thermal wave processing of lock-in thermography based on analyzing image sequences for NDT. Infrared Phys. Technol. **53**(5), 348–357 (2010)
4. Ibarra-Castanedo, C., Piau, J., Guilbert, S., e. al.: Comparative study of active thermography techniques for the nondestructive evaluation of honeycomb structures. Res. Nondestr. Eval. **20**(1) 2009
5. Halloua, H., Obbadi, A., Errami, Y., Sahnoun, S., Elhassnaoui, A.: Nondestructive inverse approach for determining thermal and geometrical properties of internal defects in CFRP composites by lock-in thermography. In : 2016 International Conference on Electrical Sciences and Technologies in Maghreb (CISTEM), pp. 1−7. IEEE (2016)
6. Sesana, R., Santoro, L., Curà, F., et al.: Assessing thermal properties of multipass weld beads using active thermography: microstructural variations and anisotropy analysis. Int. J. Adv. Manuf. Technol. **128**, 2525–2536 (2023). https://doi.org/10.1007/s00170-023-11951-8
7. An, Y.K., Kim, J.M., Sohn, H.: Laser lock-in thermography for detection of surface-breaking fatigue cracks on uncoated steel structures. Ndt E Int. **65**, 54−63 (2015)
8. Hwang, S., An, Y., Kim, J., Sohn, H.: Monitoring and instantaneous evaluation of fatigue crack using integrated passive and active laser thermography. Opt. Lasers Eng. **119**, 9–19 (2019)
9. Curà, F., Sesana, R., Corsaro, L., Mantoan, R.: Active thermography technique for barrier coatings characterization. In: IOP Conference Series: Materials Science and Engineering, vol. 1214, p. 012034 (2022)
10. Curà, F., Sesana, R., Corsaro, L., Mantoan, R.: Characterization of thermal barrier coatings using an active thermography approach. Ceramics **5**(4), 848–861 (2022)
11. Curà, F., Sesana, R., Dugand, M., Corsaro, L.: Active thermography characterization of aerogel materials for vehicle electrification. In: IOP Conference Series: Materials Science and Engineering, vol. 1275, p. 012014 (2023)
12. Curà, F., Sesana, R., Corsaro, L., Santoro, L.: La termografia attiva applicata allo studio della fatica nei materiali metallici: un caso studio. In: AIPnD 2022 - Conferenza Nazionale sulle Prove Non Distruttive, Monitoraggio e Diagnostica, pp. 19–21 (2022)
13. Straffelini, G.: Friction and Wear Methodologies for Design and Control, Springer International (2015)
14. Bhushan, B.: Modern Tribology Handbook, CRC Press (2000)
15. Maculotti, G., Goti, E., Genta, G., Mazza, L., Galetto, M.: Uncertainty-based comparison of conventional and surface topography-based methods for wear volume evaluation in pin-on-disc tribological test. Tribol. Int. **165**, 107260 (2022)
16. Bogatin, E.: Signal and Power Integrity, 2nd Edition, Prentice Hall (2009)
17. MathWorks Inc., Signal Processing Toolbox. https://it.mathworks.com/products/signal.html.